Catalysis Communications 27 (2012) 33–37

Contents lists available at SciVerse ScienceDirect

Catalysis Communications

journal homepage: www.elsevier.com/locate/catcom

Short Communication

Efficient carbon-based acid catalysts for the propan-2-ol dehydration

Vitaliy E. Diyuk *, Alexander N. Zaderko, Liudmyla M. Grishchenko, Andrii V. Yatsymyrskiy, Vladyslav V. Lisnyak

Department of physical chemistry, Chemical Faculty, Kyiv National Taras Shevchenko University, 64, Volodymyrska str., 01601 Kyiv, Ukraine

ARTICLE INFO

Article history:
Received 23 March 2012
Received in revised form 12 June 2012
Accepted 17 June 2012
Available online 23 June 2012

Keywords:
Carbon-based solid acids
Surface halogenation
Propan-2-ol dehydration

ABSTRACT

Halogenated activated carbons (AC–Hal, Hal = F, Br and Cl) used as precursors were functionalized with SO_3H groups to prepare (AC–Hal–S) solid acid catalysts. ACs obtained were subjected to chemical and elemental analysis, characterized by miscellaneous physicochemical techniques and were tested in the propan-2-ol dehydration. The high catalytic activity of AC–Hal–S (Hal = F, Cl) is attributed to the presence of F and Cl affect on the catalysts performance and stability at the operation conditions.

1. Introduction

Textural characteristics and unique surface chemistry of activated carbons (ACs) make them prospective candidates to be used for the preparation of efficient acid catalysts [1,2]. The oxidation treatment of ACs [3] can result in the formation of O-containing surface groups and the strongest acidic groups of them are carboxylic groups, whose acidity is too low relative to the most acidic sulfonic groups.

The sulfonation of carbon materials with sulfuric acid and oleum are used mainly to prepare sulfonated carbon catalysts [4–7]. The highest SO_3H groups' concentration can be obtained by sulfonation of the partly carbonized carbon materials [7]. However, solid acid catalysts obtained have a relatively low specific surface area and poor mechanical characteristics. A surface treatment with diazonium benzenesulfonic salt can be considered as an alternative route to prepare solid acid catalysts [8–10]. Thus, this route is complicated and non-selective.

Activated carbons (ACs) are characterized by advanced surface area and good mechanical properties. However, high temperature treatment of precursors at the ACs preparation stages caused a loss of surface reactivity, so the treatment with H_2SO_4 gives a minor amount of functionalized SO_3H groups. To change the ACs surface reactivity one can use surface chemical reactions for grafting halogen-containing groups and strong acidic groups, such as SO_3H.

In the present communication we reported a route to prepare solid acids catalysts, which is based on the reactivity of carbons C=C bonds. The route includes a stage of halogenation to prepare halogenated AC surfaces (AC–Hal, Hal = Br, Cl, F) as precursors. The AC–Hal obtained was functionalized with necessary moieties to form ACs with strong acidic SO_3H groups (AC–Hal–S). Functionalized solids acids (AC–Hal–S) were tested in a model propan-2-ol dehydration reaction and their performances were compared.

2. Experimental

2.1. Preparation of AC–Hal

AC prepared from *Prunus armeniaca* fruit stones was used in this study. The samples of AC with halogenated surface were obtained as follows:

(**1**) AC (5 g) was immersed in (**1a**) a bromine aqueous solution (20 g of KBr and 10 g of Br_2 in 60 ml H_2O) or in (**1b**) a dry liquid Br_2 (5 ml), and was kept at 298 K for 1 h to prepare AC–Br(1) and AC–Br(2), respectively. The brominated samples were treated with a 10% $K_2C_2O_4$ aqueous solution (200 ml) for 3 h to remove physisorbed Br_2, were washed with water and dried at 393 K;

(**2**) AC was treated in a CCl_4/Ar mixture ($C(CCl_4) = 2.03 \cdot 10^{-3}$ mol/l, GSV = 50 cm^3/min) at 723 K for 1.5 h to prepare AC–Cl. The AC–Cl was then flushed with Ar for another 1 h to remove physisorbed CCl_4 and cooled down to 298 K;

(**3**) AC–Cl (5 g) was immersed in a solution for fluorination (25 mmol KF and 20 mmol of 18-crown-6 in 50 ml of CH_3CN) at 298 K for 24 h to prepare AC–Cl–F. The AC–Cl–F obtained was washed with distilled water and dried at 393 K.

2.2. Preparation of AC–Hal–S

The Hal-atoms were substituted for the S-containing groups as follows. AC–Hal (1 g) was immersed in 5 ml of an aqueous solution of (**4**)

* Corresponding author at: Chemical Faculty, Kyiv National Taras Shevchenko University, Kyiv 01601, Ukraine. Tel./fax: +380 44 2581241.
E-mail address: dve@univ.kiev.ua (V.E. Diyuk).

1566-7367/$ – see front matter © 2012 Elsevier B.V. All rights reserved.
doi:10.1016/j.catcom.2012.06.018

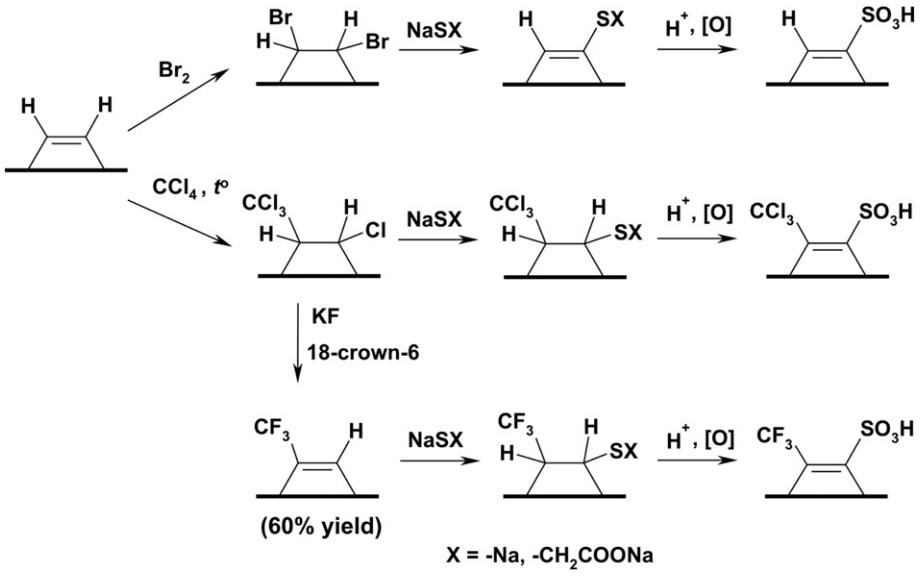

Fig. 1. The routes used to prepare the AC–Hal and AC–Hal–S and the proposed structure of surface functionalities.

25% $NaSCH_2COONa$ or (**5**) 20% Na_2S to prepare AC–Hal–(1) or AC–Hal–S(2), respectively. The samples obtained were transferred into an autoclave glass beaker to be heated for 12 h at 393 K to form S*X*-adducts. The ACs with S*X*-adducts were immersed in a 25% HCl aqueous solution (100 ml) at 373 K for 2 h, washed with water and then treated with a 30% H_2O_2 solution (50 ml) for 3 h. The AC–Hal–S samples obtained after the wet oxidation were washed with water and dried at 393 K. A sample AC–S(1), to be used for the comparison, was prepared by the same technique omitting the halogenation stage. Fig. 1 illustrates the routes used and schematized structures of surface functionalities.

The stages of ACs functionalization are based on strategic application of organic chemistry reactions as follows: electrophilic addition of Br_2 [11] or of CCl_4 [12] to double C=C bonds with formation of AC–Br and AC–Cl, respectively; nucleophilic substitution of Cl in CCl_3 groups with F to form AC–Cl–F; nucleophilic substitution of active surface halogen in AC–Hal (Hal = Cl, Br) with NaS*X* (*X* = CH_2COONa, Na) or nucleophilic addition of NaS*X* to double bonds activated with CF_3 groups (AC–Cl–F) to form S*X* adducts; hydrolysis and oxidation with H_2O_2 of S*X* adducts to form SO_3H groups. Nucleophilic substitution of surface Br with NaS*X* (*X* = CH_2COONa, Na) is accompanied with HBr elimination and C=C bond formation. Earlier, a principal possibility of the bromine electrophilic addition and its nucleophilic substitution with amines, alcohols and thiols was shown for Norit activated carbon in Ref. [11].

2.3. Catalysts characterization

The N_2 adsorption–desorption analysis was performed for degassed at 423 K ACs samples on a Micromeritics ASAP 2010 volumetric adsorption system at 77 K. The specific surface area (S_{BET}) was determined using the BET method. The total pore volume (V_S) was estimated from the amount of N_2 adsorbed at a relative pressure of 0.95.

The elemental analysis (E.A.) of samples was performed with Oxford Inca 350 energy dispersive X-ray spectrometer mounted on a Jeol JSM-6490 scanning electron microscope. Titrimetric Volgard's (Br, Cl) and Eschke's (total S content) methods were used for chemical analysis (C.A.) of functionalized ACs.

The ACs surface chemistry was analyzed by X-ray photoelectron spectroscopy (XPS, Kratos 800 Ultra System, MgKα = 1253.6 eV) and by thermal desorption analysis. The concentrations of CO, CO_2 and SO_2 (C_{CO}, C_{CO_2}, C_{SO_2}) evolved due to thermal destruction of the ACs surface groups were determined by temperature-programmed desorption with IR spectrometric registration of gaseous desorption products (TPD-IR). An apparatus combining TG/DTG analyzer and Specord 400 IR-spectrometer was used for all the TPD-IR studies. The sample (0.1 g) stored in a quartz pan, which is situated in a custom quartz tubular reactor placed inside an electrical furnace, was heated in a flow of a purge Ar gas (GSV = $7 \cdot 10^{-5}$ m^3/min). The temperature was increased from 303 K to 1073 K with a rate of 10 K/min and the sample weight change was recorded in a form of TG/DTG profiles. Evolved gases, which are transferred with the Ar flow from the furnace heated area into the flow cell of the IR-spectrometer, were tested on-line, and TPD-IR profiles were registered. The IR intensities related to the concentrations of CO, CO_2 and SO_2 were calibrated daily with diluted gases mixtures. For the temperature-programmed desorption, ultra-high-purity Ar, was used as the inert purge gas, since besides desorption no oxidation could occur. The value of C_{SO_2} was considered as a measure of SO_3H groups content. The MAS ^{19}F NMR spectra were recorded on an Avance 400 NMR spectrometer at 298 K. The concentration of strong acid sites (C_A) was determined by acid/base pH-metric titration. The quantum-chemical (QC) computation (see Appendix A for procedure) was performed to mimic qualitatively the affect of substitutes on the ACs relative acidity.

Table 1
The textural properties (S_{BET}, V_S), results of E.A. and C.A., C_{CO} and C_{CO_2} determined by TPD-IR.

Sample	S_{BET}, m^2/g	V_S, cm^3/g	E.A.					C.A.	TPD-IR	
			Element content, at. %						C_{CO}, mmol/g	C_{CO_2}, mmol/g
			C	O	Br	Cl	F	C_{Hal}, mmol/g		
AC	1350	0.45	95.9	4.1	–	–	–	–	0.76	0.12
AC–Br(1)	1085	0.41	87.2	11.1	1.7	–	–	0.62	1.41	0.25
AC–Br(2)	1050	0.40	88.9	9.3	1.8	–	–	0.52	1.44	0.29
AC–Cl	950	0.36	86.3	7.2	–	6.5	–	4.60	1.34	0.88
AC–Cl–F	985	0.38	86.0	7.4	–	3.7	2.9	2.52(Cl);1.91(F)	1.36	0.91

Table 2
Binding energies (E_b) of the chemical states of C, O, Cl, Br and S and the states relative content (in parenthesis, in %) for selected ACs.

Sample	E_b, eV										
	C 1s				O 1s		Cl $2p_{3/2}$		Br $3p_{3/2}$	S $2p_{3/2}$	
	C—C	C—O	C=O	O—C=O	O—I (C=O+S=O)	O—II (C—O+S—O)	C—Cl	CCl_3	C—Br	SH	SO_3H
AC	284.4 (70.4)	285.6 (14.4)	286.6 (12.4)	288.7 (2.8)	532.4 (43.4)	533.8 (56.6)					
AC–Br(1)	284.4 (70.1)	285.6 (16.6)	286.9 (9.6)	288.3 (3.7)	532.2 (39.7)	533.8 (60.3)			183.6 (100)		
AC–Cl	284.4 (72.2)	285.6 (17.3)	286.7 (7.7)	288.1 (2.8)	532.4 (36.3)	533.8 (63.7)	200.1 (82.1)	201.2 (17.8)			
AC–Br(1) –S(1)	284.4 (70.2)	285.5 (16.6)	286.6 (9.0)	288.4 (4.2)	532.3 (41.0)	533.8 (59.0)				163.8 (9.3)	168.9 (90.7)

2.4. Catalysts test

The catalytic activity of ACs obtained was examined in a flow reactor at atmospheric pressure (see Appendix A for details). As the propan-2-ol catalytic dehydration over ACs functionalized with strong acidic groups gave propene mainly and diisopropyl ether traces [13,14], the propan-2-ol conversion to propene (α) and the reaction rate (r) were calculated by means of Eqs. (1) and (2), respectively

$$\alpha = \frac{C(C_3H_6)}{C_0(C_3H_7OH)}, \quad (1)$$

where $C(C_3H_6)$ is the propene outlet concentration, and $C_0(C_3H_7OH)$ is the propan-2-ol inlet concentration equal to $1.07 \cdot 10^{-3}$ mol/l, and

$$r = C(C_3H_6) \cdot GSV, \quad (2)$$

where GSV is the gas velocity rate equals 45 cm^3/min. The propan-2-ol dehydration reaction heating-cooling cycles were carried out to evaluate catalyst deactivation. The temperature at 100% conversion of propan-2-ol to propene ($T_{100\%}$) was used as a measure of the catalytic activity. The evolution of $T_{100\%}$ value from I to III cycle was used to estimate the catalysts deactivation.

3. Results and discussion

3.1. Characterization of AC–Hal

Table 1 summarizes the textural properties, result of analysis and TPD-IR data for the AC and AC–Hal.

The initial AC is characterized by significant amount of phenolic, carbonyl groups (evolved CO) and carboxyl groups (evolved CO_2) [3]. The halogenation of ACs leads to decrease of S_{BET} (by 20–30%) and V_S (by 7–20%). This observation can indicate on the preferential micropore surface functionalization with Hal. The content of Hal in the AC–Cl and AC–Cl–F samples is 8–10 times higher than that in the AC–Br ones. The bromination is realized by the electrophilic addition of Br_2 to double C=C bonds. In contrast to the bromination, the formation of C—Cl and CCl_3 groups (*cf.*, Table 2) was realized at the high temperature chlorination by the reaction of CCl_4 with C=C bonds [12]. Alternatively, $Cl^{\bullet}$ and $CCl_3^{\bullet}$ radicals can react with the AC surface centers, e.g. OH or C—H. The formation of surface CCl_3 groups by the radical reaction causes the high content of Hal in the AC–Cl (>4.5 mmol/g).

F is able to substitute only about 40% of Cl in the AC–Cl (*cf.*, Table 1). Fig. 2 shows a typical MAS ^{19}F NMR spectrum of AC–Cl–F sample.

The main peak registered at −64 ppm/$CFCl_3$ was assigned to the surface AC–CF_3 groups in accordance with data of [15,16]. Signals at −117 and −162 ppm/$CFCl_3$ were attributed to CF groups in the aromatic and aliphatic fragments of carbon matrix, respectively. The partial substitution of Cl by F is realized due to the difference in the reactivity of CCl_3 groups, which depends on the nearest-neighbor groups. The reactivity of CCl_3 groups increases if electron acceptor groups (e.g. carbonyl, activated aryl, lactonic or carboxylic groups) are located closely to them.

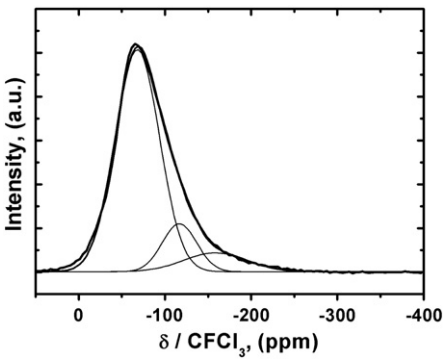

Fig. 2. ^{19}F MAS NMR spectrum of AC–Cl–F–S(1) (spinning rate of 10 kHz).

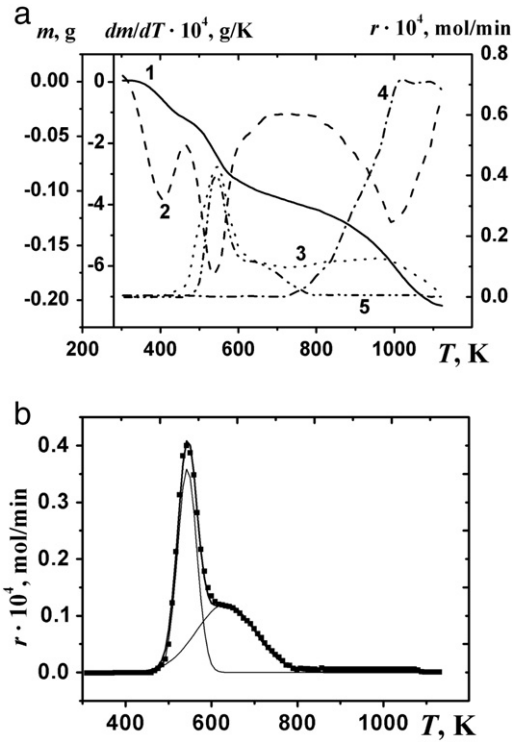

Fig. 3. Typical TG (1), DTG (2) and TPD-IR profiles of CO_2 (3), CO (4) and SO_2 (5) desorption (a); deconvoluted TPD profile of SO_2 (b).

Table 3
The textural properties (S_{BET}, V_S), results of C.A., $C(SO_2)$ and $T_{max,\ (1)}$, $T_{max,\ (2)}$ from the TPD-IR data, the concentration of strong acid centers (C_A) and $T_{100\%}$ at I–III heating–cooling cycles over modified ACs.

Sample	S_{BET}, m^2/g	V_S, cm^3/g	C.A.	TPD-IR			C_A, mmol/g	$T_{100\%}$, K		
			$C(S)$, mmol/g	$C(SO_2)$, mmol/g	$T_{m(1)}$, K ($C_1 \cdot 10^{-4}$, mol/g)	$T_{m(2)}$, K ($C_2 \cdot 10^{-4}$, mol/g)		I	II	III
AC–S(1)	1280	0.44	0.22	0.16	583 (0.8)	643 (0.8)	0.14	531	577	592
AC–Br(1)–S(1)	1120	0.42	0.36	0.21	568 (1.3)	653 (0.8)	0.20	514	529	544
AC–Br(2)–S(1)	1075	0.41	0.36	0.21	568 (1.2)	653 (0.9)	0.18	521	543	553
AC–Br(2)–S(2)	1055	0.40	0.55	0.13	523 (0.4)	623 (0.9)	0.09	525	546	562
AC–Cl–S(1)	980	0.37	0.45	0.42	543 (2.1)	643 (2.1)	0.41	479	485	492
AC–Cl–S(2)	960	0.36	0.56	0.24	533 (1.2)	633 (1.2)	0.23	488	494	498
AC–Cl–F–S(1)	1050	0.39	0.50	0.29	533 (0.4)	638 (2.5)	0.29	488	492	494

As significant amounts of CO_2 and especially CO were registered by TPD-IR for the AC–Hal, consequently, significant ACs surface oxidation is accompanied with the halogenation (Table 1). It was found, if the XPS data for the initial AC and AC–Hal are compared, that the ratio of (C—O)/(C=O) forms increases in the AC–Hal; the latter corresponds to the formation of phenolic groups (*cf.*, Table 2). Hydrolysis of the most active surface Br or Cl can cause the formation of phenolic groups (up to 0.7 mmol/g). In summary, it is clearly seen that the ACs can be functionalized with 0.5–4.5 mmol/g of Hal-containing groups through the halogenations routes used.

3.2. Characterization of AC–Hal–S

XPS data confirm the formation of sulfonic (SO_3H) groups grafted on the AC–Hal–S. The main sulfur XPS peak S($2p_{3/2}$) at 168.9 eV (*cf.*, Appendix A, Table 2) was assigned to the surface SO_3H groups. The peak at 163.8 eV was assigned to the rest of SH surface groups. The XPS data on O(1s) are not informative for investigation of the concentration of SO_3H groups. The binding energies for the oxygen in S=O and S—O of SO_3H groups are close to those in C=O and C—O of oxygen functional surface groups of the active carbon [17]. So, O(1s) core level XP spectrum can be deconvoluted on the two components from O—I (S=O and C=O) and O—II (S—O and C—O) type oxygen [17]. The formation of sulfonic acid groups of up to 0.5 mmol/g gives two oxygen forms S=O and S—O in 2:1 ratio; the latter should lead to increase of the total content of O—I form. This effect is observed experimentally as the relative amount of the O—I form increases from 39.7% for AC–Br(1) to 41.0% for AC–Br(1)–S(1).

Fig. 3a represents typical TG/DTG, TPD-IR profiles registered for the AC–Hal–S samples. The TPD profile of SO_2 that evolved from the grafted SO_3H groups can be deconvoluted into two Gaussian components (Fig. 3b).

Two maximum of SO_2 thermal desorption ($T_{max,\ (1)}$, $T_{max,\ (2)}$) registered by TPD-IR (Table 3) were assigned to two forms of SO_2. These forms can be associated with SO_3H groups grafted in the meso-/macropores and in the micropores, respectively.

The concentration of SO_3H groups in the AC–Br–S determined form the TPD-IR data is 1.7–4.2 times lesser than the total amount of S (C.A.) and 2.5–4 times lesser than the total amount of Br in the AC–Br (Table 3).

The SO_3H groups' low concentration is caused by 1) partial hydrolysis of the surface Br groups at the treatment of AC-Br with basic Na_2S or $NaSCH_2COONa$ reagents or/and by 2) partial hydrolysis of the S*X*-adduct. The higher SO_3H groups concentrations of 0.42 and

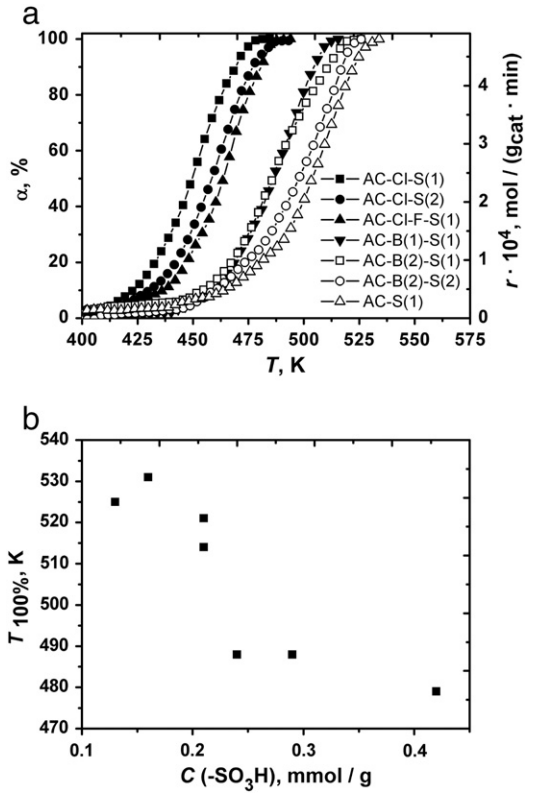

Fig. 4. Conversion of propane-2-ol to propene with the temperature (a) and T100% against the concentration of functionalized SO_3H groups in the ACs (b).

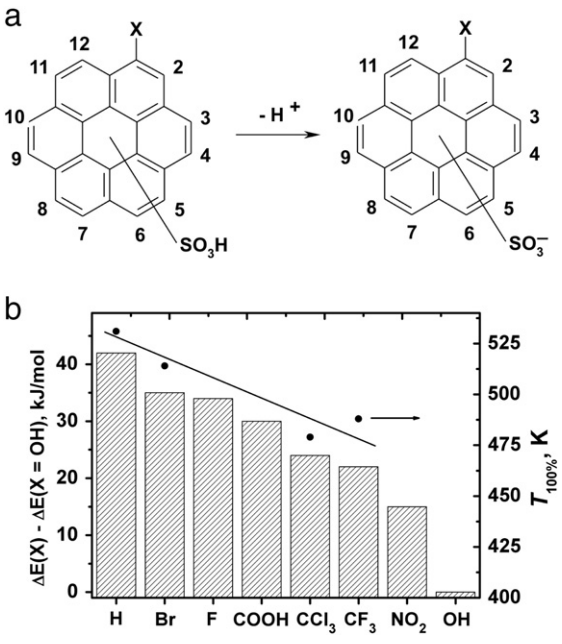

Fig. 5. The protonated ($C_{24}H_{10}XSO_3H$) and deprotonated ($C_{24}H_{10}XSO_3^-$) forms of a model object used for the difference in energy estimation (a), correlation plot of $\Delta E(X) - \Delta E(OH)$ and $T_{100\%}$ with substituent *X*.

0.29 mmol/g were achieved if use the AC–Cl and the AC–Cl–F precursors, respectively. This fact can be explained by the higher concentration of active Hal and by the acceptor properties of CCl_3 and CF_3 groups facilitate the stage of the Na_2S or $NaSCH_2COONa$ addition. The solid acids prepared contain up to 0.42 mmol/g of the strong acidic group. These data are in a good agreement with SO_2 concentration determined from the TPD-IR (Table 3).

3.3. Catalytic properties

Fig. 4a shows that all modified ACs samples exhibit a high activity level and convert 100% propane-2-ol to propene. The standard industrial grade strong acid catalyst amberlyst-15 WET was also tested in this reaction. It was found that propan-2-ol converted to propene over amberlyst-15 at 403 K with a yield of 77%. At higher temperature α value decreases from 77% at 403 K to 65% at 428 K (see Appendix A for details). The catalyst deactivation is caused by the thermal degradation of the surface SO_3H groups.

The catalyst activity and the reaction rates ($r \cdot 10^4$ mol g^{-1} min^{-1} at 470 K) decrease in a sequence AC–Cl–S(1) (4.36) > AC–Cl–S(2) (3.69), AC–Cl–F–S(1) (3.24) > AC–Br(2)–S(1) (1.10), AC–Br(1)–S(1) (1.05), AC–Br(2)–S(2) (0.82) > AC–S(1) (0.61).

The dependence of catalytic activity of studied samples (in fact $T_{100\%}$) against the concentration of functionalized SO_3H groups has a complicated character that cannot be trivially interpreted as the two parameter dependence (Fig. 4b). In general the catalytic activity increases ($T_{100\%}$ decreases) with increase of the concentration of functionalized SO_3H groups.

According to the data obtained one can suggest that the highest activity of the AC–Cl–S(1), AC–Cl–S(2) and AC–Cl–F–S(1) samples is realized due to affect of CCl_3 and CF_3 groups on the proton affinity of SO_3H groups.

The effect of substituents on the ACs relative acidity was modeled with DFT QC method for a model object, and the difference in the energy ($\Delta E(X)$) of the protonated ($C_{24}H_{10}XSO_3H$) and deprotonated ($C_{24}H_{10}XSO_3^-$) forms (Fig. 5a) was calculated (*cf.*, Appendix A for QC data). It was found that minimal $\Delta E(X)$ is for X = OH. Fig. 5b shows that the presence of the nearest CCl_3 and CF_3 groups decreases $\Delta E(X) - \Delta E(OH)$ and so increases the deprotonation of SO_3H groups. The lowest $T_{100\%}$ values are found for the ACs containing CCl_3 and CF_3 groups; this confirms for the some extent the suggestion done. The $\Delta E(X) - \Delta E(OH)$ values decrease with X in a sequence H > Br > F > COOH > CCl_3 > CF_3 > NO_2 > OH. $T_{100\%}$ values decrease in a similar way for selected X-substituents. So, the $\Delta E(X) - \Delta E(OH)$ values could be used to estimate the influence of a substituent on the activity of carbon solid acids functionalized with SO_3H groups.

The value of $T_{100\%}$ for the functionalized ACs increases from I to III heating–cooling cycle at the operation condition (Table 3). The highest deactivation, which is caused by the partial destruction of active centers of the catalysts, is observed for the AC–Br(2)–S(2) and AC–S(1). The chlorinated and especially fluorinated ACs preserve the performance for at the least the next 5 heating–cooling cycles. The catalysts deactivation occurs due to the reduction of S in the SO_3H groups with the AC matrix; the latter is accompanied with evolving of SO_2 gas. The surface of chlorinated and fluorinated AC samples is more chemical inert to the oxidation due to the deactivation of reductive surface centers at the stage of the radical chlorination.

4. Conclusions

A novel synthetic route for the preparation of carbon-based solid acids was elaborated. The halogenation of AC with subsequent reaction of the AC–Hal with $NaSCH_2COONa$ or Na_2S allow obtaining ACs with up to 0.5 mmol/g of the strong acid SO_3H groups. The carbon-based solid acids prepared show a high activity level in the model reaction of catalytic propan-2-ol dehydration to propene. The most efficient catalysts are that obtained from the fluorinated and chlorinated ACs. The halogen-containing surface moieties not only increase the catalytic activity of the AC-based solid acids, but also increase the reactive groups thermal stability in the case of AC–Cl–S(1) and of AC–Cl–F–S(1) to the utmost.

Appendix A. Supplementary data

Supplementary data to this article can be found online at http://dx.doi.org/10.1016/j.catcom.2012.06.018.

References

[1] B.V.S.K. Rao, K. Chandra Mouli, N. Rambabu, A.K. Dalai, R.B.N. Prasad, Catalysis Communications 14 (2011) 20–26.
[2] J. Bedia, R. Ruiz-Rosas, J. Rodriguez-Mirasol, T. Cordero, Journal of Catalysis 271 (2010) 33–42.
[3] W. Shen, Zh. Li, Y. Liu, Recent Patents on Chemical Engineering 1 (2008) 27–40 and references herein.
[4] J.H. Clark, V. Budarin, T. Dugmore, R. Luque, D.J. Macquarrie, V. Strelko, Catalysis Communications 9 (2008) 1709–1714.
[5] X. Moa, D.E. Lopez, K. Suwannakarn, Y. Liu, E. Lotero, J.G. Goodwin Jr., C. Lu, Journal of Catalysis 254 (2008) 332–338.
[6] A.M. Dehkhoda, A.H. West, N. Ellis, Applied Catalysis A: General 382 (2010) 197–204.
[7] B.V.S.K. Rao, K.C. Mouli, N. Rambabu, A.K. Dalai, R.B.N. Prasad, Catalysis Communications 14 (2011) 20–26.
[8] L. Geng, G. Yu, Y. Wang, Y. Zhu, Applied Catalysis A: General 427–428 (2012) 137–144.
[9] R. Liu, X. Wang, X. Zhao, P. Feng, Carbon 46 (2008) 1664–1669.
[10] F. Barroso-Bujans, J.L.G. Fierro, S. Rojas, S. Sanchez-Cortes, M. Arroyo, M.A. Lopez-Manchado, Carbon 45 (2007) 1669–1678.
[11] V.L. Budarin, J.H. Clark, S.J. Tavener, K. Wilson, Chemical Communications 23 (2004) 2736–2737.
[12] K. Tanemura, T. Suzuki, Y. Nishida, T. Horaguchi, Tetrahedron 66 (2010) 2881–2888.
[13] J. Bedia, J.M. Rosas, J. Marquez, J. Rodriguez-Mirasol, T. Cordero, Carbon 47 (2009) 286–294.
[14] V.E. Diyuk, L.N. Grishchenko, V.K. Yatsimirskii, Theoretical and Experimental Chemistry 44 (2008) 331–336.
[15] K. Gatoh, K. Takeda, M.M. Lerner, Y. Sueishi, S. Maruyama, A. Gato, M. Tansho, S. Ohki, K. Hashi, T. Shimizu, H. Ishida, Carbon 49 (2011) 4059–4073.
[16] H. Touhara, F. Okino, Carbon 49 (2000) 241–267.
[17] C. Petit, K. Kante, T.J. Bandosz, Carbon 48 (2010) 654–667.